

Ecological Performance Analysis of an Integrated Proton Exchange Membrane Fuel Cell and Thermoelectric Devices

Yuewu Huang*, Hui Ding, Yufei Zou

College of Environmental Science and Engineering, Donghua University, Shanghai 201620, China

*E-mail: huangyaowu@sina.com

Received: 22 October 2019 / Accepted: 30 December 2019 / Published: 10 February 2020

Proton exchange membrane fuel cells (PEMFCs) are promising fuel cells, however, they exhaust waste heat while operating. In order to recycle the waste heat, a novel model coupling a thermoelectric generator (TEG) and a thermoelectric cooler (TEC) with a PEMFC is established. The thermodynamic and electrochemical irreversible losses including Thomson effect are considered. A set of analytical formulas are derived for overall equivalent power output under different scenarios. Parametric study is presented in this work. The ecological coefficient of performance (ECOP) which represents the equivalent output power of the unit loss of availability is employed as an objective function for system evaluation. The results show that, compared with the individual fuel cell, the maximum power density and ECOP of the hybrid system are increased by 1.42% and 4.47%, respectively. Comparing two cases with or without considering Thomson effect, it can be concluded that the Thomson effect has negative impacts on system performance to a certain extent.

Keywords: fuel cell; PEMFC; thermoelectric; ecological optimization; Thomson effect

1. INTRODUCTION

Electric vehicles (EVs) are developing rapidly. According to *Global EV Outlook 2019* published by International Energy Agency, in 2018, the number of the global electric car exceeded 5.1 million. Fuel cells have been used in electric vehicles including passenger cars and other various transport applications[1]. Faced with the energy shortage, fuel cells have been considered as an ideal alternative for traditional energy conversion devices due to less pollution and high conversion efficiency [2, 3].

Among the existing fuel cells, proton exchange membrane fuel cell (PEMFC) can be used in automobiles or portable electronic equipment because of quick start and favorable power-to-weight ratio, making it one of the most promising fuel cells [4, 5]. Researches have been conducted to study on the performance of PEMFC for optimization, including in the aspects of catalyst [6], material [7, 8],

geometric construction [9-11], working conditions [12-14], utilization of waste heat [15-17] and so on. The recovery of waste heat to enhance the performance of fuel cells has attracted attention worldwide [18]. Zhao et al.[19] proposed a typical fuel cell–heat engine hybrid system, and found the heat transfer irreversibility in the heat engine affected the system performance. Unlike fuel cells with high operating temperature which can integrate with heat engines, PEMFCs have much lower temperature, so the waste heat generated is inadequate to drive heat engines [15]. At present, PEMFCs tend to be integrated with heat pump [15], thermoelectric coolers [16, 17], adsorption chiller [20] and so on. Thermoelectric devices are superior to conventional thermal energy devices in the aspects of reliability and maintenance [21, 22]. Moreover, TEG can convert thermal energy into electricity via Seebeck effect, and TEC can utilize the electricity for cooling via Peltier effect [23]. Integrating fuel cells with thermoelectric devices have been an alternative for heat recovery and cogeneration. A new cogeneration system consisting of a direct carbon fuel cell and a two-stage TEG was established by Liu et al., and the results showed that the maximum power output density was 50% larger than that of the stand-alone fuel cell [24]. Wu et al. developed an integrated phosphoric acid fuel cell and thermoelectric device system for power and cooling cogeneration, both power density and efficiency of the hybrid system were improved compared to the stand-alone PAFC [21]. As a result, integrating a PEMFC and TEG/TEC makes sense.

A hybrid system formed by a PEMFC and TEG-TEC to improve the system performance is established in this work. Some irreversible losses including Thomson effect are taken into account. The system can recycle the waste heat from PEMFC to drive TEG and TEC to gain power and cooling capacity. Current density, power density and optimal range of the proposed system have been researched based on the ecological coefficient of performance (ECOP). To provide theoretical basis for practical design of this system, effects of some design parameters as well as Thomson effect on the system have been investigated.

2. SYSTEM DESCRIPTION

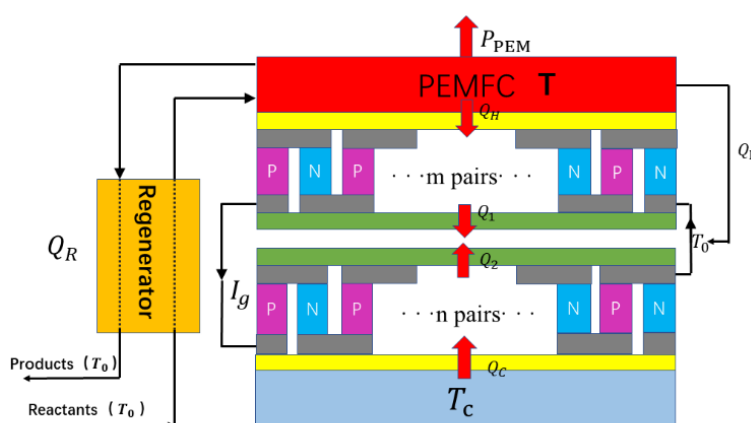


Figure 1. Schematic diagram of a cogeneration system integrating a PEMFC with thermoelectric devices

The diagram of the proposed system coupling a PEMFC with a TEG, a TEC and an irreversible regenerator is presented by Figure 1.

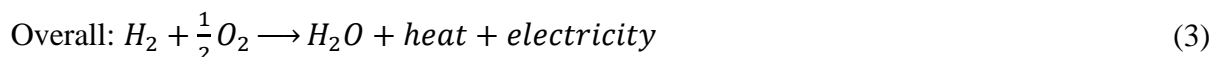
The PEMFC is working at the temperature of T . Electric power converted from chemical energy in the PEMFC is written as P_{PEM} . Waste heat is generated in this process as well. Some of that waste heat Q_H is absorbed by the TEG module to produce electric current I_g via Seebeck effect. With I_g maintained in the circuit, the TEC module absorbs heat Q_c from the cooling room at the temperature of T_c via Peltier effect. Some of that waste heat, Q_L , is dissipated to the ambient air at the temperature of T_0 . Meanwhile, the products from the PEMFC can preheat the reactants by regenerator and generate waste heat, Q_R . Q_1 and Q_2 are the heat dissipated into the ambient environment, respectively, from the TEG module and TEC module.

The model has been simplified as follows:

- 1) The PEMFC and thermoelectric devices are operating in a steady state;
- 2) The working temperature and working pressure of the PEMFC are maintained at fixed values;
- 3) No reactants are left in the reaction of the PEMFC;
- 4) The external irreversible losses between TEG-TEC and cooling space are neglected;
- 5) Thermoelectric elements won't conduct electricity and heat with the surroundings, and electric current flows in the direction of the leg in a thermoelectric element.

2.1 PEMFC

PEMFC is supplied with hydrogen and oxygen to drive the reactions and produces liquid water, heat and electricity. The reaction formulas are given as below:



The thermodynamic relationship of the PEMFC can be presented as:

$$-\Delta H = -\Delta G - T\Delta S \quad (4)$$

where ΔG is Gibbs free energy change, ΔS is entropy change, ΔH is enthalpy change in the reaction, and $\Delta H = I\Delta h/(n_e F)$, where I is the working current of the PEMFC, Δh is molar enthalpy change, n_e is the number of electrons, F is Faraday constant.

The open circuit voltage E under standard conditions can be derived from the Nernst equation as below [25, 26]:

$$E = 1.229 - 8.5 \times 10^{-4}T - 298.15 + 4.3085 \times 10^{-5} \times T \left(\ln P_{H_2} + \frac{1}{2 \ln P_{O_2}} \right) \quad (5)$$

where P_{H_2} and P_{O_2} are the partial pressures of H_2 and O_2 .

Based on the energy conservation, the actual voltage V from the PEMFC can be obtained by subtracting the voltage losses, including concentration loss, V_{con} , activation loss, V_{act} , and Ohmic loss, V_{ohmic} , from the Nernst voltage, E . The voltage losses can be calculated by:

$$V_{\text{act}} + V_{\text{con}} + V_{\text{ohmic}} = \frac{\lambda_a + \lambda_c}{\lambda_a \lambda_c} \frac{RT}{n_e F} \ln \frac{j}{j_0} + j \left(\beta_1 \frac{j}{j_{\text{max}}} \right)^{\beta_2} + j \frac{t_{\text{mem}}}{\sigma_{\text{mem}}} \quad (6)$$

where $\sigma_{\text{mem}} = (0.005139\lambda_{\text{mem}} - 0.00326) \exp \left[1268 \left(\frac{1}{303} - \frac{1}{T} \right) \right]$ and $j_0 = 1.08 \times 10^{-21} \exp(0.086 \times T)$. λ_a and λ_c are the anode and cathode charge transfer coefficients of the

electrodes, respectively. j represents the current density which is the ratio of current I to effective electrode area A . j_0 and j_{max} are current exchange density and limiting current density in the PEMFC. R refers to the universal gas constant. t_{mem} and σ_{mem} are the membrane thickness and proton conductivity. β_1 and β_2 are the concentration coefficients. λ_{mem} is membrane humidity.

The actual voltage, power output and efficiency of the PEMFC can be derived:

$$V = E - (V_{act} + V_{con} + V_{ohmic}) \tag{7}$$

$$P_{PEM} = VI = [E - (V_{act} + V_{con} + V_{ohmic})]I \tag{8}$$

$$\eta_{PEM} = \frac{P_{PEM}}{-\Delta H} = \frac{1}{-\Delta H} [E - (V_{act} + V_{con} + V_{ohmic})]I \tag{9}$$

2.2 TEG-TEC

The thermoelectric devices in the hybrid system refer to a TEG and a TEC. The number of elements of the TEG is m and that of TEC is n . Each element has a P-type and an N-type semiconductor leg, and these elements are in series connection. Neglecting the external irreversibility, the main causes for the irreversibility inside the thermoelectric elements are Joule heat, heat-conduction loss and heat loss due to Thomson effect. Consequently, the heat transfer balance equations of the thermoelectric devices can be presented as:

$$Q_H = \alpha_h m I_g T - 0.5 m I_g^2 R_1 + m K_1 (T - T_0) - \frac{\tau_1 m I_g (T - T_0)}{2} \tag{10}$$

$$Q_1 = \alpha_0 m I_g T_0 + 0.5 m I_g^2 R_1 + m K_1 (T - T_0) + \frac{\tau_1 m I_g (T - T_0)}{2} \tag{11}$$

$$Q_2 = \alpha_0 n I_g T_0 + 0.5 n I_g^2 R_2 - n K_2 (T_0 - T_c) - \frac{\tau_2 n I_g (T_0 - T_c)}{2} \tag{12}$$

$$Q_c = \alpha_c n I_g T_c - 0.5 n I_g^2 R_2 - n K_2 (T_0 - T_c) + \frac{\tau_2 n I_g (T_0 - T_c)}{2} \tag{13}$$

where α_h , α_0 and α_c are the Seebeck coefficients related to T , T_0 and T_c . $R = \frac{\rho_P l_P}{S_P} + \frac{\rho_N l_N}{S_N}$ is the inner resistance of thermoelectric element, where the subscript 1 represents TEG and 2 represents TEC, respectively. ρ refers to resistivity of thermoelectric element; I_g is the electricity flowing through the TEG-TEC; l and S are, respectively, the length and cross-sectional area of the semiconductor leg. $K = \frac{k_P S_P}{l_P} + \frac{k_N S_N}{l_N}$ is the thermal conductance of an element, where k is the thermal conductivity, the subscript P or N represents P-type or N-type semiconductor leg. τ is Thomson coefficient.

Table 1. Properties of Bi₂Te₃

Parameters	Values
α ($V \cdot K^{-1}$)	$2 \times (22224.0 + 930.6T - 0.9905T^2) \times 10^{-9}$
$\rho_N = \rho_P$ ($\Omega \cdot m$)	$(5112.0 + 163.4T_m + 0.6279T_m^2) \times 10^{-10}$
$k_N = k_P$ ($W \cdot m^{-1} \cdot K^{-1}$)	$(62605.0 - 277.7T_m + 0.413T_m^2) \times 10^{-4}$
τ ($V \cdot K^{-1}$)	$2 \times (930.6T_m - 1.981T_m^2) \times 10^{-9}$

Considering the operating temperature of TEG-TEC, Bi₂Te₃ is applied as the thermoelectric material, and the temperature dependent properties of it are presented in Table 1 [27, 28].

T_m is the average temperature of thermoelectric elements. $T_{m_1} = (T + T_0)/2$ and $T_{m_2} = (T_c + T_0)/2$, respectively, refer to the average temperature of TEG module and TEC module.

Parameter χ can be defined to represent the ratio of the numbers of the elements in TEG and TEC:

$$\chi = \frac{m}{n} = \frac{(\alpha_0 T_0 - \alpha_c T_c) - \tau_2(T_0 - T_c) + I_g R_2}{(\alpha_h T - \alpha_0 T_0) - \tau_1(T - T_0) - I_g R_1} \quad (14)$$

Based on Eq. (10), Eq. (13) and Eq. (14), the coefficient of performance (*COP*) and cooling capacity (Q_c) can be expressed as:

$$COP = \frac{Q_c}{Q_H} = \frac{\alpha_c I_g T_c - 0.5 I_g^2 R_2 - K_2(T_0 - T_c) + \frac{\tau_2 I_g (T_0 - T_c)}{2}}{\alpha_h I_g T - 0.5 I_g^2 R_1 + K_1(T - T_0) - \frac{\tau_1 I_g (T - T_0)}{2}} \cdot \frac{1}{\chi} \quad (15)$$

$$Q_c = \frac{m}{\chi} \cdot [\alpha_c I_g T_c - 0.5 I_g^2 R_2 - K_2(T_0 - T_c) + \frac{\tau_2 I_g (T_0 - T_c)}{2}] \quad (16)$$

To make TEG-TEC work normally, both *COP* and Q_c should be positive, i.e. $COP > 0$ and $Q_c > 0$. Thus, the interval of working current of TEG-TEC can be expressed as: $I_a < I_g < I_b$, where

$$I_a = \frac{[0.5\tau_2(T_0 - T_c) + \alpha_c T_c] - \sqrt{[0.5\tau_2(T_0 - T_c) + \alpha_c T_c]^2 - 2R_2K_2(T_0 - T_c)}}{R_2} \quad (17)$$

$$I_b = \frac{\alpha_h T - \alpha_0 T_0 - \tau_1(T - T_0)}{R_1} \quad (18)$$

The equivalent power output of TEG-TEC can be expressed as:

$$P_{td} = Q_c |1 - T_0/T_c| \quad (19)$$

2.3 Regenerator

The regenerative loss caused by thermal resistances can be written as:

$$Q_R = K_{re} A_{re} (1 - \xi)(T - T_0) \quad (20)$$

where K_{re} is heat transfer coefficient of the regenerator. A_{re} is the regenerative heat transfer area. ξ is the regenerative efficiency.

2.4 Hybrid system

Due to temperature difference, part of the heat generated by the electrochemical reaction will leak into the environment, which can be expressed as:

$$Q_L = K_L A_L (T - T_0) \quad (21)$$

where K_L and A_L are heat leak coefficient and heat leak area.

The quantity of heat transferred from PEMFC to TEG can be derived as below:

$$Q_H = -\Delta H - P_{PEM} - Q_R - Q_L \\ = -\frac{A\Delta h}{2F} \left[(1 - \eta_{PEM})j - \frac{2Fc_1(T - T_0)}{-\Delta h} - \frac{2Fc_2(T - T_0)}{-\Delta h} \right] \quad (22)$$

where $c_1 = K_{re}A_{re}(1 - \beta)/A$, $c_2 = K_L A_L/A$ are the temperature-independent regenerative loss coefficient and the heat leak coefficient.

From Eq. (10) and Eq. (22), the following equation can be obtained:

$$I_g = \frac{1}{R_1} [2\alpha_h T - \tau_1(T - T_0)] - \frac{1}{R_1} \sqrt{\left[\alpha_h T - \frac{\tau_1(T - T_0)}{2}\right]^2 + R_1 \left\{ 2K_1(T - T_0) + \frac{A\Delta h}{Fm} \left[(1 - \eta_{PEM})j + \frac{2F(T - T_0)(c_1 + c_2)}{\Delta h} \right] \right\}}$$

(23)

When thermoelectric devices work normally, substituting I_a and I_b into Eq. (23), the minimum and maximum current density of thermoelectric devices, j_a and j_b , respectively, can be derived. Therefore, the overall equivalent power output can be expressed as:

$$P = \begin{cases} P_{PEM} + P_{td} & (j_a < j < j_b) \\ P_{PEM} & (j \leq j_a \text{ or } j \geq j_b) \end{cases}$$

(24)

The definition of ECOP is the ratio of power output to the loss rate of availability [29, 30], and can be written as:

$$ECOP = P/T_0\sigma$$

(25)

where σ is the entropy increase rate.

According to Eq. (24) and Eq. (25), the ECOP of the hybrid system can be derived:

$$ECOP = \frac{P_{PEM} + P_{td}}{T_0(\sigma_{cell} + \sigma_{td})}$$

(26)

where σ_{cell} and σ_{td} are given as:

$$\sigma_{cell} = \frac{-\Delta G - P}{T_0} - \frac{Q_H}{T_0} + \frac{Q_H}{T}$$

(27)

$$\sigma_{td} = -\frac{Q_H}{T} + \frac{Q_H + Q_c}{T_0} - \frac{Q_c}{T_c}$$

(28)

3.RESULTS AND DISCUSSION

3.1 Performance analysis and optimization of the system

With the mathematical model, the numerical solution of PEMFC/TEG-TEC hybrid system is given out. Parameters used in modeling are shown in Table 2 [16, 17, 31].

Figure 2 shows the curves of the power densities of stand-alone fuel cell, TEG-TEC and hybrid system, where P^* , P_{PEM}^* and P_{td}^* represent the corresponding power densities of the proposed hybrid system, PEMFC and thermoelectric devices, respectively. Power density is the ratio of power output to effective electrode area. It can be seen from Figure 2 that the thermoelectric devices only works in the region of $j_a < j < j_b$, and outside of this region, the curve of $P^* \sim j$ is overlapped with the curve of $P_{PEM}^* \sim j$. All these power densities first increase with j to attain the maximum values and then decrease. It should be noted that the corresponding current j_c at maximum P^* is always different from the current j_d at P_{PEM}^* .

Table 2. Parameters used in modeling

Parameters	Values
universal gas constant, R ($J \cdot mol^{-1} \cdot K^{-1}$)	8.314
number of electrons, n_e	2
ambient temperature, T_0 (K)	290
temperature of cooled space, T_c (K)	273
Faraday's constant, F ($C \cdot mol^{-1}$)	96485
operating temperature of PEMFC, T (K)	363
partial pressure of H_2 , P_{H_2} (atm)	2.305
partial pressure of O_2 , P_{O_2} (atm)	0.4068
molar enthalpy change of the electrochemical reactions, Δh ($kJ \cdot mol^{-1}$)	-284.0
cathode charge transfer coefficient, λ_c	1.364
anode charge transfer coefficient, λ_a	1.116
concentration coefficients, $\beta_1; \beta_2$	0.5; 1.88
limiting current density, j_{max} ($A \cdot cm^{-2}$)	1.503
membrane humidity, λ_{mem}	15.89
membrane thickness, t_{mem} (cm)	0.018
number of thermoelectric elements on the top, m	12
comprehensive parameters, $c_1; c_2$ ($W \cdot m^{-2} \cdot K^{-1}$)	0.1; 0.1

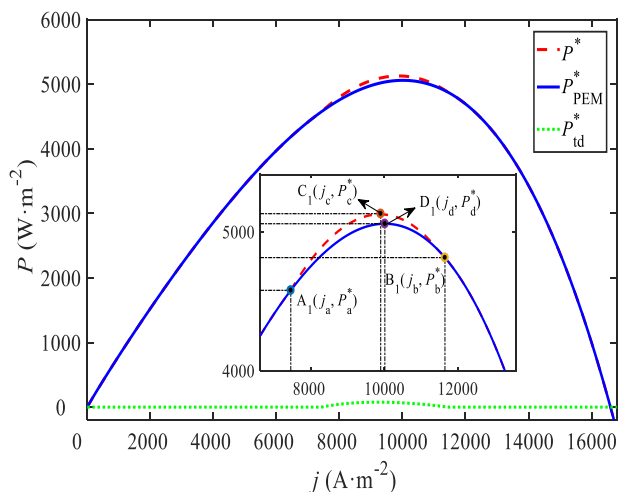


Figure 2. Curves of the P of the PEMFC, TEG-TEC and hybrid system varying with the current density

The ECOPs of the stand-alone fuel cell and the hybrid system with respect to the power density has been presented in Figure 3. According to the definition of ECOP, a higher ECOP represents a better performance. It is reasonable to use ecological function for environmental friendly system [29, 32]. To evaluate the system performance with ecological criterion, Figure 2 is combined with Figure 3, and results can be obtained as follows: the optimal region of the proposed hybrid system are $P_a^* < P^* < P_c^*$ and $E_c < ECOP < E_a$. The corresponding optimal region of current density is $j_a < j < j_c$. By numerical calculation, taking stand-alone PEMFC as the objective, the maximum power density can be derived as $P_d^*=5058.7W/m^2$, and the corresponding ECOP is 0.76. As for hybrid system, the peak of power density, P_c^* , is $5131W/m^2$, and the corresponding ECOP is 0.79. Comparing the data mentioned above, it shows

that the peak value of power and the corresponding ECOP of hybrid system are 1.42% and 4.47% larger than those of the stand-alone PEMFC, respectively. It can be seen that the system performance enhancement is not obvious in the short term, but in the aspect of whole life cycle, the low maintenance cost can compensate for the initial construction cost. Zhang et al. [2] integrated the TEG-TEC with a SOFC (solid oxide fuel cell) to harvest waste heat, and found the maximum power density was 2.3% higher than that of the single fuel cell. In view of the high operating temperature and large amount of waste heat of SOFC, the performance enhancement of PEMFC is considerable. Consequently, utilizing TEG-TEC is an effective way to reuse waste heat from PEMFC to improve the system performance.

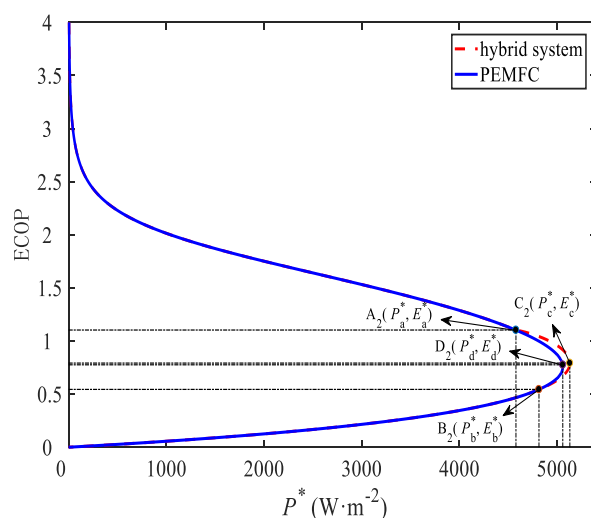


Figure 3. Curves of the ECOP of the PEMFC and hybrid system varying with the power density

3.2 Effects of operating temperature T

Figure 4 reveals the influences of T on the hybrid system. As j is fixed, both P^* and ECOP increase with the increased T , especially in the region of $j > 8000 \text{ A} \cdot \text{m}^{-2}$. Moreover, j_a, j_b, j_c and $\Delta j = j_a - j_b$ are getting larger as T rises. Since the molecules in the fuel cell reactions have a higher kinetic energy with increased temperature, the probability and the fraction of collisions bringing about reaction are dramatically related to temperature T . Although a higher temperature contributes to more heat loss and heat leak, it improves the conductivity of ions in the electrolyte and decreases the overpotential loss, which promotes the actual power output of PEMFC. The same rule can be found from PAFC-TEG/TEC system proposed by Wu et al. [21] in 2017. Besides, the larger temperature difference results in a better performance of thermoelectric devices. In conclusion, the energy obtained due to a higher temperature far outweighs the energy loss, so it's feasible to optimize the performance of hybrid system by increasing operating temperature. In practical use, the cost of high temperature should be taken into consideration to propose an economical energy conversion system.

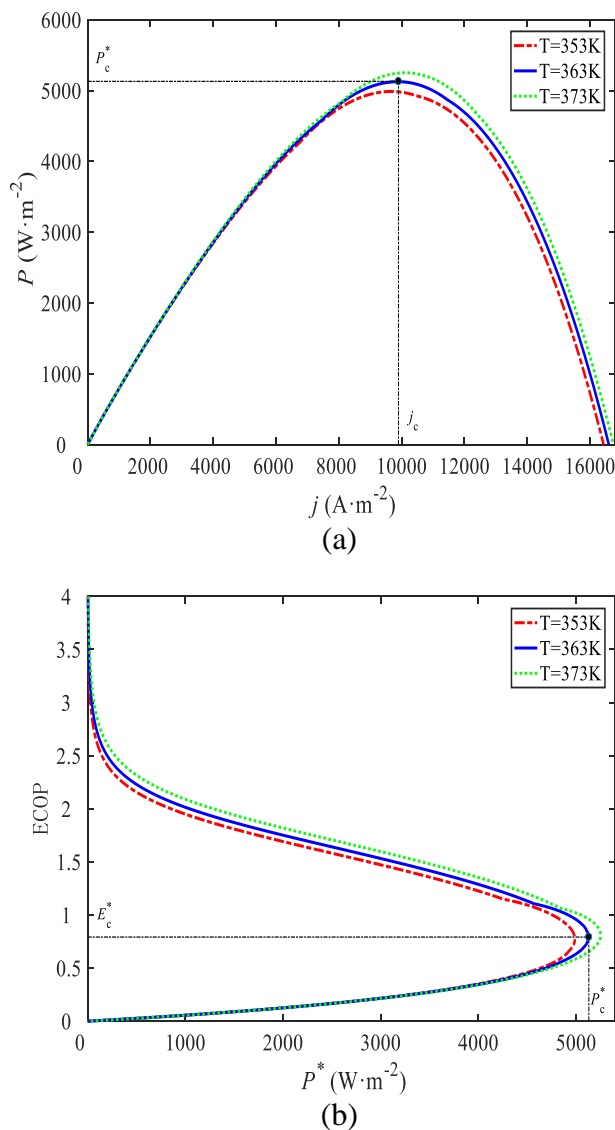


Figure 4. Effects of T on the (a) power density, (b) ECOP of the hybrid system

3.3 Effects of operating pressure p

Due to the influences on the characteristics of the PEMFC and heat transfer process from the PEMFC to thermoelectric devices, the operating pressure p is an important parameter. As is shown in Figure 5, similar to the influence of T , for a given current density, both P^* and ECOP show an upward tendency with the increase of p , which is more obvious in the region of higher current density. According to the numerical calculation, both j_a and j_b ascend with p , while Δj decreases with p . The reasons are that higher operating pressure can accelerate the concentration of reactions, degrade concentration of polarization and gain voltage. However, with the raised pressure, more power is needed to compress the fuel and oxide at the entrance, which will make the system more complicated and costly. Hence, the choice of p is usually 1 atm. And this is different from the residential micro-combined cooling heating and power system driven by PEMFC, whose optimum p is 2 atm [33].

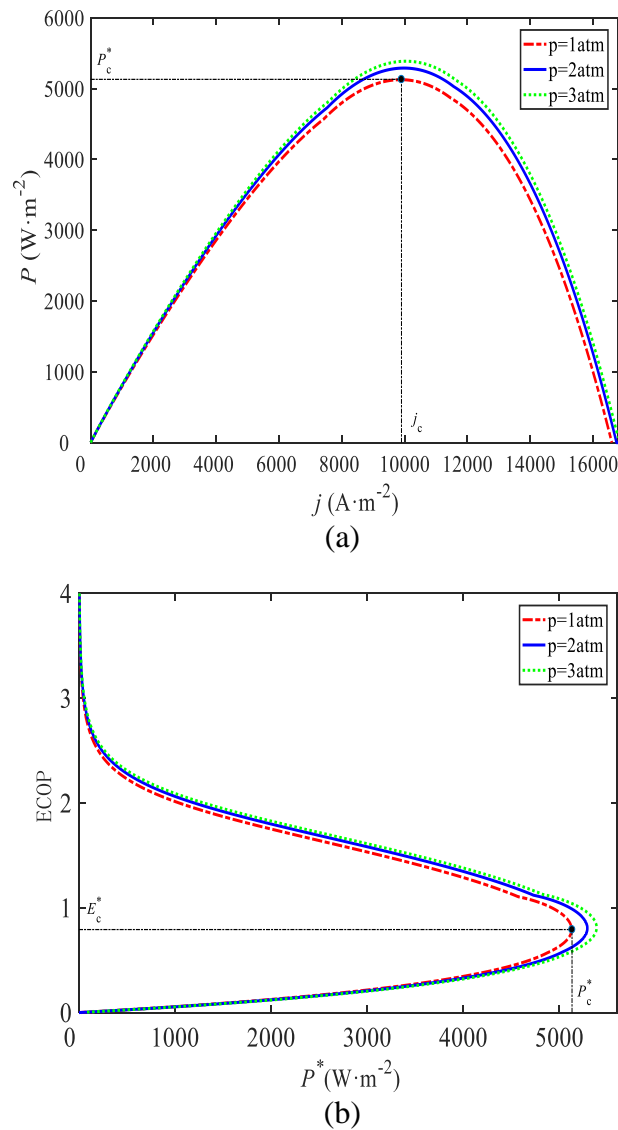


Figure 5. Effects of p on the (a) power density, (b) ECOP of the hybrid system

3.4 Effects of number of thermoelectric elements

Unlike operating temperature and pressure, the number of thermoelectric elements only has effects on hybrid system in the region of $j_a < j < j_b$. From Figure 6, it can be seen that j_a , j_b , Δj and P_{td}^* are ongoingly reduced with the decrease of m , on the contrary, ECOP decreases as m becomes larger. P_c^* first mounts up to its peak value and then declines when m is added. The explanation for this phenomenon is that loss rate of availability rises with the increase of m . When m rises to some extent, the improvement of P_{td}^* is unable to compensate for the loss of P_{PEM}^* . M. Ebrahimi et al. [20] presented a PEMFC-based model, and found the increasing number of TEGs decreased the efficiency of the hybrid system, however, by using particular number of TEG modules, the electricity produced by TEGs increased from 0.55W to 16.5W. As a result, m should be chosen carefully to maximize P_c^* .

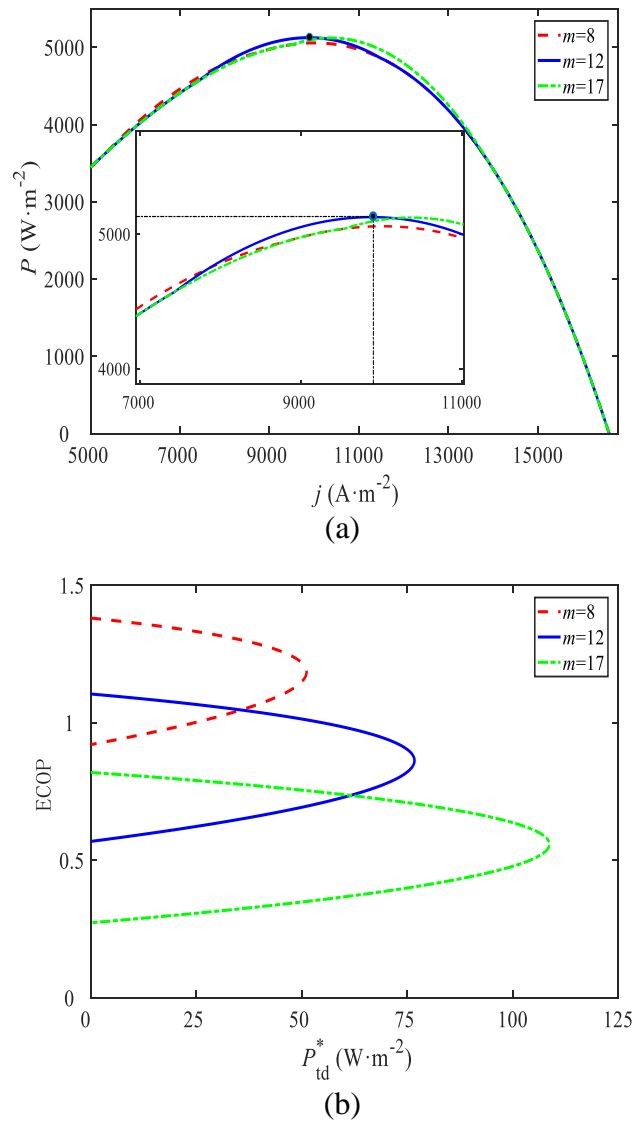


Figure 6. Effects of m on the (a) power density, (b) ECOP of the hybrid system

3.5 Effects of Thomson effect

Feng et al. [34] investigated the effects of Thomson effect on the TEG-TEC device, and the results showed the cooling capacity was decreased by 27% due to Thomson effect. Because of the negative impact on TEG-TEC, Thomson effect can degrade the hybrid system performance. Impacts of Thomson effect on the working region, power density and ECOP have been shown in Figure 7. It indicates that the working region and ECOP of hybrid system as well as the power density of TEG-TEC are all decreased due to Thomson effect, and this is more obvious in the region of higher current density. Adopting the method of numerical calculation to compare the cases with or without considering Thomson effect, it is evident that the P_c^* and ECOP of hybrid system are reduced by 1.11% and 4.8%, respectively, when Thomson effect is considered. Hence, Thomson effect has negative effects on the system performance to some degree.

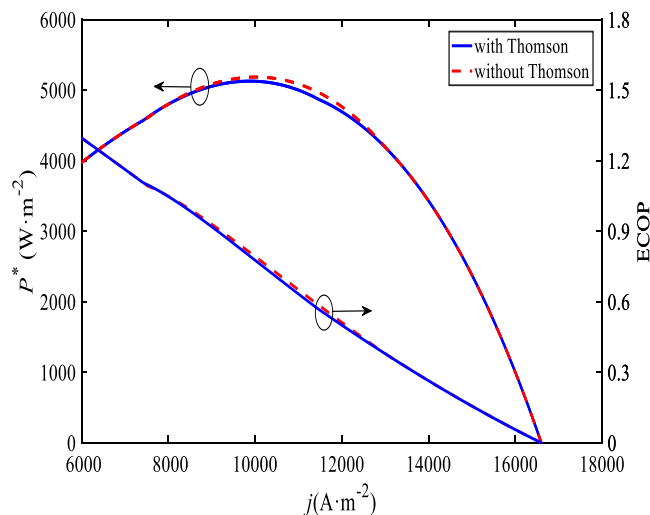


Figure 7. Effects of Thomson effect on the performance of the hybrid system

4. CONCLUSIONS

An effective way to recycle waste heat from a fuel cell is to integrate with thermoelectric devices. To evaluate the performance of a thermodynamically and electrochemically irreversible hybrid system with Thomson effect, which is mainly composed of a PEMFC, a TEG and a TEC, an ecological optimization criterion using ECOP as objective functions has been performed. The optimal intervals of current, power density and ECOP for the system performance enhancement have been determined. Effects of some parameters on the proposed system are studied by parametric analyses. Results show that both higher operating temperature and pressure can improve the performance, especially when the current density is large. Unlike operating temperature and pressure, the number of thermoelectric elements only has effects on hybrid system in the certain region. With the increased number of thermoelectric elements, ECOP increases monotonically while P_c^* reaches the summit and then declines. There exists an optimal value for the number of thermoelectric elements to maximize P_c^* . The simulation indicates that P_c^* and ECOP of the hybrid system with Thomson effect are decreased by 1.11% and 4.8%, respectively, compared to the system without Thomson effect. Hence, Thomson effect can degrade the system performance in some ways and should be noted in practical design. These results can provide some information for practical application of similar systems.

ACKNOWLEDGEMENTS

This paper is supported by the National Natural Science Foundation of China (Project No. 51078068).

References

1. I. E. Agency, "Global EV Outlook 2019: scaling-up the transition to electric mobility," International Energy Agency 2019, Available: <https://apo.org.au/node/243056>, Accessed on: Access date.
2. H. Zhang, W. Kong, F. Dong, H. Xu, B. Chen, and M. Ni, *Energy Convers. Manage.*, 148 (2017)

- 1382.
3. S. Wu, H. Zhang, and M. Ni, *Energy*, 112 (2016) 520.
 4. A. Alaswad, A. Baroutaji, H. Achour, J. Carton, A. Al Makky, and A. G. Olabi, *Int. J. Hydrogen Energy*, 41 (2016) 16499.
 5. H.-W. Wu, *Applied Energy*, 165 (2016) 81.
 6. Y.-B. Park, E. You, C. Pak, and M. Min, *Electrochim. Acta*, 284 (2018) 242.
 7. M. Langemann, D. L. Fritz, M. Müller, and D. Stolten, *Int. J. Hydrogen Energy*, 40 (2015) 11385.
 8. S. Flick, M. Schwager, E. McCarthy, and W. Mérida, *Applied Energy*, 129 (2014) 135.
 9. X. Zeng, Y. Ge, J. Shen, L. Zeng, Z. Liu, and W. Liu, *Int. J. Heat Mass Transfer*, 105 (2017) 81.
 10. C. Castelain, Y. Lasbet, B. Auvity, and H. Peerhossaini, *International Journal of Thermal Sciences*, 101 (2016) 181.
 11. E. G. Karvelas, D. G. Koubogiannis, A. HatziaPOSTOLOU, and I. E. Sarris, *Renewable Energy*, 93 (2016) 269.
 12. Z. Liu, X. Zeng, Y. Ge, J. Shen, and W. Liu, *Int. J. Heat Mass Transfer*, 111 (2017) 289.
 13. A. C. Olesen, S. H. Frensch, and S. K. Kær, *Electrochim. Acta*, 293 (2019) 476.
 14. K. Subin and P. K. Jithesh, *Sustainable Energy Technologies and Assessments*, 27 (2018) 17.
 15. X. Chen, Y. Wang, and Y. Zhou, *International Journal of Electrical Power & Energy Systems*, 63 (2014) 429.
 16. M. Ebrahimi and E. Derakhshan, *Energy Convers. Manage.*, 171 (2018) 507.
 17. M. Hasani and N. Rahbar, *Int. J. Hydrogen Energy*, 40 (2015) 15040.
 18. X. Zhang, Y. Pan, L. Cai, Y. Zhao, and J. Chen, *Energy Convers. Manage.*, 144 (2017) 217.
 19. Y. Zhao and J. Chen, *J. Power Sources*, 186 (2009) 96.
 20. M. Ebrahimi and E. Derakhshan, *Energy Convers. Manage.*, 180 (2019) 269.
 21. M. Wu, H. Zhang, J. Zhao, F. Wang, and J. Yuan, *International Journal of Refrigeration*, 89 (2018) 61.
 22. Y. Huang, *Energy Convers. Manage.*, 50 (2009) 1444.
 23. S. Manikandan and S. C. Kaushik, *Cryogenics*, 67 (2015) 52.
 24. J. Liu, *International Journal of Electrochemical Science*, (2019) 3701.
 25. X. Lai, R. Long, Z. Liu, and W. Liu, *Energy*, 147 (2018) 578.
 26. W. A. N. W. Mohamed and M. H. M. Kamil, *Energy Convers. Manage.*, 124 (2016) 543.
 27. H. Nami, A. Nemat, M. Yari, and F. Ranjbar, *Appl. Therm. Eng.*, 124 (2017) 756.
 28. S. Manikandan and S. C. Kaushik, *Energy*, 100 (2016) 227.
 29. Y. Üst, B. Sahin, and A. Kodak, *Journal of the Energy Institute*, 78 (2005) 145.
 30. P. A. Ngouateu Wouagfack and R. Tchinda, *International Journal of Refrigeration*, 40 (2014) 404.
 31. P. Yang, H. Zhang, and Z. Hu, *Int. J. Hydrogen Energy*, 41 (2016) 3579.
 32. E. Açıkkalp, *Energy Convers. Manage.*, 132 (2017) 432.
 33. X. Chen, G. Gong, Z. Wan, L. Luo, and J. Wan, *Int. J. Hydrogen Energy*, 40 (2015) 10647.
 34. Y. Feng, L. Chen, F. Meng, and F. Sun, *J. Non-Equilib. Thermodyn.*, 43 (2018) 75.